HIFiRE Re-entry Observation Using an Image-Based Visual Servoing System

Razmi Khan [1], David Buttsworth [2], Ben Upcroft [1]

[1] *The Centre of Hypersonics,*
The University of Queensland, Brisbane, 4072, QLD, Australia
[2] *Faculty of Engineering and Surveying*
University of Southern Queensland, Toowoomba, 4350, QLD, Australia

Summary: This paper presents an image based visual servoing system that is intended to be used for tracking and obtaining scientific observations of the HIFiRE vehicles. The primary aim of this tracking platform is to acquire and track the thermal signature emitted from the surface of the vehicle during the re-entry phase of the mission using an infra-red camera.

The implemented visual servoing scheme uses a classical image based approach to identify and track the target using visual kinematic control. The paper utilizes simulation and experimental results to show the tracking performance of the system using visual feedback. Discussions on current implementation and control techniques to further improve the performance of the system are also explored.

Keywords: HIFiRE, Visual Servoing, Machine Vision, Visual Feedback

Introduction

HIFiRE is the Hypersonic International Flight Research Experiment - a joint venture between the Australian Defence, Science and Technology Organization and the US air force. The intent of the research is to ultimately achieve sustained hypersonic flight through a series of experiments which involve rocket-launching scramjet engines in a sequence of progressively challenging trajectories. There are considerable engineering challenges remaining in the area of scramjet-sustained hypersonic flight, particularly relating to thermal loads and supersonic combustion. The remaining flights within the HIFiRE program provide an excellent opportunity to glean additional data in these areas through ground-based observations. For example, emission spectroscopy through remote observation of the scramjet exhaust plumes could provide an additional diagnostic tool for scramjet combustion efficiency analysis. Furthermore, remote thermal IR imaging of the vehicle would also be possible because of the high surface temperatures which are achieved during flight.

Efforts to monitor the surface temperatures in hypersonic flight have previously been demonstrated on the HYTHIRM project [11-13]. This project successfully acquired high resolution thermal radiation images from the heat shield for several NASA Space Shuttle re-entries. The optical equipment mounted on an airborne platform used a hybrid tracking approach. Initial acquisition was done using computer aided techniques that would initially acquire the target within the field of view of the cameras. Once acquired in the FOV of the tracking camera, a mirror which reflected the radiation emitted from the heat shield surface was steered manually to keep track of the target centred in the image plane. Such position based systems typically require accurate equipment calibrations with the system being prone to target acquisition inaccuracies due to calibration errors and target position offsets. Manual

operation can be challenging especially when the target is at a large distance and high resolution imaging is required. Under these conditions, erroneous manual pointing of the camera equipment can arise and may cause failure to acquire the necessary data. To address this problem, an automated image based tracking approach is proposed to robustly obtain the emitted thermal radiation for the atmospheric re-entry of the HIFiRE test vehicle.

The proposed technique to track the re-entry involves implementation of classical image based visual feedback control based on experiments carried out by Corke et al. [8]. The approach uses a technique that would detect a manually chosen target between frames of a video sequence and track using a 2 axis pan and tilt robot as it moves across the field of view of the camera. Previously Hutchinson et al. [7] and Papanikolopoulos et al. [4] provided the fundamentals of visual servoing and discussed the control issues that affect stability and performance.

This paper discusses the vision and control strategies that are being developed for tracking the HIFiRE test vehicle on its hypersonic re-entry phase of the mission. System modelling will also be introduced to aid in selecting appropriate gains that would achieve a desired response to the system. Provisions for the further improvement of tracking performance of the system using feed forward control strategies will also be discussed. Note that the proposed thermal/IR camera in Figure 1 is for demonstration purposes only. Integration of suitable IR cameras with the proposed system is yet to be addressed.

The layout of the paper includes an outline of the equipment setup proposed and formation of an image Jacobian discussed in the following section. In section ‘Visual Feedback Control’ we model the feedback system and discuss the analysis and system timing. Following this we show the system tracking performance results and a comparison between the simulation and the actual system being developed. Finally, we conclude with a brief discussion on further improving the tracking performance of the system and implementation for the upcoming HIFiRE re-entry.

Visual Servoing Architecture

In this section we introduce the prototype equipment and setup. We also present the image Jacobian and the simplifications employed to analyze the control.

Equipment Setup

The prototype robot is a Directed Perception PTU-47-17 high speed pan and tilt unit. This unit hosts a ‘Flea 2’ black and white Point Grey camera capable of running at 30Hz. Figure 1 shows the mounting of this camera on the right and the proposed thermal camera on the left of the robot payload bracket. Initial indoor and outdoor target tracking tests were conducted using a 6mm focal length lens on the tracking camera. Note that the actual cameras and lenses that will be used for tracking and signal acquisition from HIFiRE have not been finalized. The equipment in the present work is adopted for the purpose of system analysis and demonstration. A typical desktop CPU interfaces with the camera and robot using an IEEE 1394b standard interface and serial respectively. All vision processing and robot movement tasks were handled by a C program written in Microsoft Visual Studios in a Windows based environment.

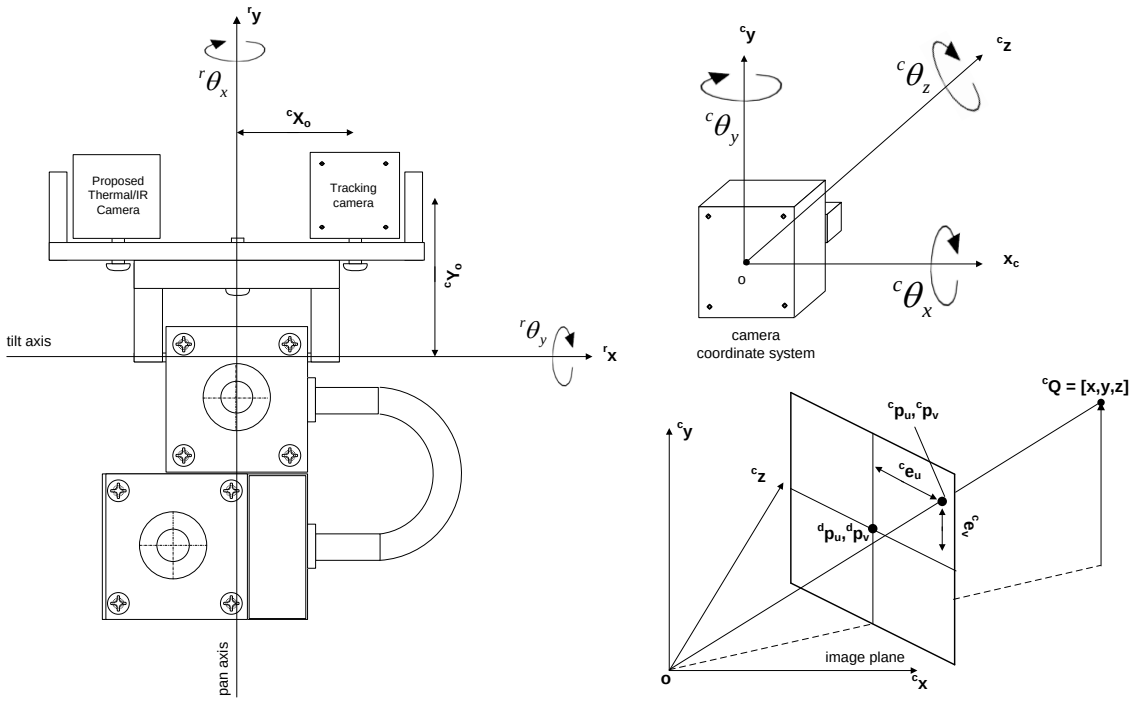

Fig. 1. A prototype of the robot (left) is shown with a 2-DOF rotational movement with proposed camera mountings. Figures on the right top and bottom demonstrate the camera coordinate system in terms of which all modelling will be shown and a typical target position on the image plane with an error condition respectively

Image Jacobian

For an end effector mounted camera setup, tracking a target requires a known relationship between the change in target position on the image plane to the change in robot pose. Using a pin hole camera model and a perspective geometric relationship between the target and the camera, an image Jacobian can be derived. Corke et al. [8] and Haralick et al. [5] show a detailed derivation of this transformation. The resultant image Jacobian for a point ${}^{c}\boldsymbol{O} = [x_c, y_c, z_c]$ expressed in the camera coordinates can be written as,

$$\dot{\boldsymbol{p}} = \boldsymbol{J} * \dot{\boldsymbol{r}}$$

which can be expressed as a matrix,

$$\begin{bmatrix} \dot{p}_u \\ \dot{p}_v \end{bmatrix} = \begin{bmatrix} \frac{f}{z} & 0 & \frac{-p_u}{z} & \frac{-p_u p_v}{f} & \frac{f^2 + p_u^2}{f} & -p_v \\ 0 & \frac{f}{z} & \frac{-p_v}{z} & \frac{-f^2 - p_v^2}{f} & \frac{p_u p_v}{f} & p_u \end{bmatrix} \begin{bmatrix} T_x \\ T_y \\ T_z \\ \omega_x \\ \omega_y \\ \omega_z \end{bmatrix}$$

where $\dot{\boldsymbol{p}}$ is the velocity of the image feature with p_u and p_v the target coordinates on the image plane. T_x, T_y, T_z and $\omega_x, \omega_y, \omega_z$ are translational and rotational velocities of the end effector respectively. f is the focal length of the camera lens in pixels.

The Jacobian, $\boldsymbol{J}$ can be simplified into two equations for a 2 DOF robot rotational motion only. For pure rotational motion in the pitch and yaw axis the Jacobian matrix can be reduced to the following equations,

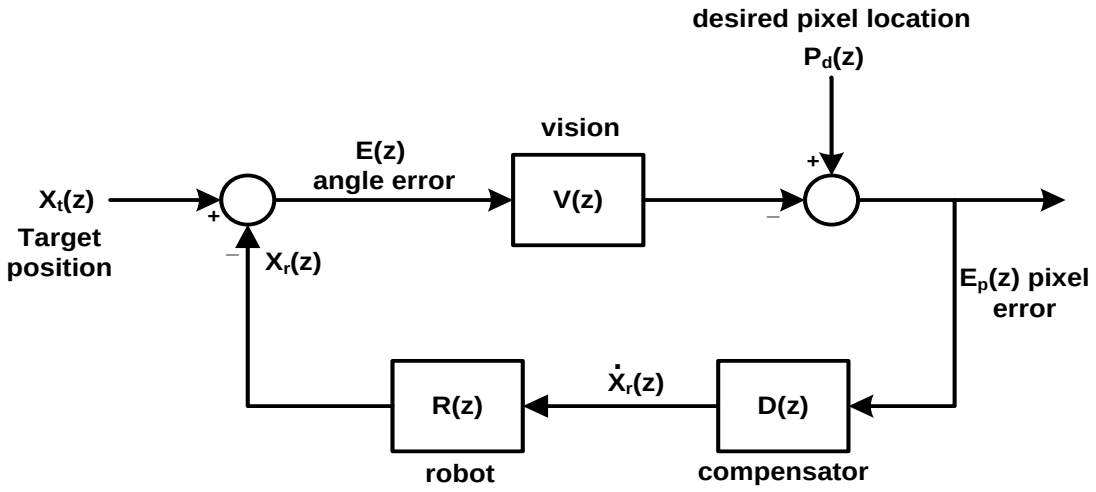

Fig. 2. Block diagram of the feedback control system. Note that the above figure shows single axis control only

$$\dot{p}_u = \frac{f^2 + p_u^2}{f}\omega_y \text{ and } \dot{p}_v = \frac{f^2 + p_v^2}{f}\omega_x$$

In forming the equations above, a few approximations need to be addressed. The off axis mounting of the tracking camera leads to the introduction of the two offset terms ${}^cX_o$ and ${}^cY_o$ (as shown in Figure 1) when transforming the robot coordinate system to the camera coordinates. The yawing and pitching motions about the *y* and *x* axes introduces robot translation velocities. Assuming that the distance of the object being tracked is ${}^c\boldsymbol{O} = [x_c, y_c, \infty]$ and the offset terms ${}^cX_o$, ${}^cY_o \approx 0$, the translational motion induced can be approximated as zero.

Vision algorithm

Visual servoing is typically classified into two phases. The first task requires the target to be identified between frames of a video sequence. The identified target (in this case a point object) is then centered within the frame by moving the end effector mounted camera. High resolution imagery of the re-entry vehicle is possible using a large focal length lens on the thermal cameras. Depending on the selected observation location with respect to the re-entering vehicle, the apparent size of the target will increase as the object moves closer to the imaging equipment. This may require the use of target identifying vision algorithms such as CAMSHIFT that take into consideration the increasing size of the object on the image plane. However, for simplicity all analysis and results discussed in this paper use targets as point objects and implements the Lucas Kanade optical flow pyramidal approach to acquire the target in subsequent frames [1].

Visual Feedback Control

In this section we present the visual feedback control scheme that will be used throughout our analysis and experimental sections. A high level architecture is shown in Figure 2. To simplify the analysis, the system will be assumed as a single axis system. Target movement is assumed only about the y axis that corresponds to the horizontal line on the 2D image plane. To

validate this assumption the 2-DOF prototype robot uses identical pitch and yaw axis stepper motors. Due to the insignificant weight and offset distances of the cameras from the centre of each of the rotational axis, the moment of inertia I_c can be approximated as zero.

System modelling

The prototype system is a single rate system that runs at the video update rate of 30Hz. The robot controller rate is programmable and is to set the same frequency. As shown by Corke et al. [6] a single rate discrete time system can be modelled primarily in terms of delay. Each module of the system is therefore represented as a function in discrete *z* domain notation.

The primary objective of the system is to detect and fixate as the target moves. Therefore, the output of the model shown in Figure 2 describes the image plane pixel error $E_p(z)$ for a given target motion $X_t(z)$. The desired pixel location $P_d(z)$ is always at the centre of the image plane with coordinates ${}^d p_u$, ${}^d p_v$. The discrepancies between the robot position and the target position in the image plane yields the error signal $E(z)$, in radians.

The compensator on the feedback path applies a fixed proportional gain to the image error velocity output $\dot{X}_r(z)$. The vision system, $V(z)$ is modelled as a single sample period delay, K_{lens}/z. The delay can vary between one to three frames depending on the number of cameras on the bus and the resolution of the cameras. K_{lens} is an approximation of the lens gain for a particular focal length set on the camera. For small angular target changes per sample period this gain can be approximated as the focal length of the lens in pixels/rad. The focal length was measured experimentally using the Camera Calibration Toolbox in Simulink MATLAB.

The compensator here is a purely proportional feedback gain. Together with the image Jacobian, the feedback provides the robot with a velocity command. The proportional gain K_p was chosen using analytical and experimental techniques to provide a critically damped response. These gains are analytically derived and discussed in the analysis section.

The robot $R(z)$ is composed of a combination of three parts, a robot dynamics $R_d(z)$ described in the next section, an integrator $z/z\text{-}1$, and a single frame delay $1/z$. The robot starts to change pose as soon as a command reaches the controller via serial communication and therefore moves in real time. The delay is introduced since the change in robot position is only sensed by the system at the next shutter event.

Robot dynamics

The robot acceleration and velocity information is provided by the manufacturer and is programmable to user defined settings.

The velocity of the robot $\dot{X}_r(z)$ is divided into two segments: velocities above and below base velocity V_b as shown in Figure 3. For velocities above the base speed the robot takes time to accelerate to the requested velocity and decelerate before reaching the requested pose.

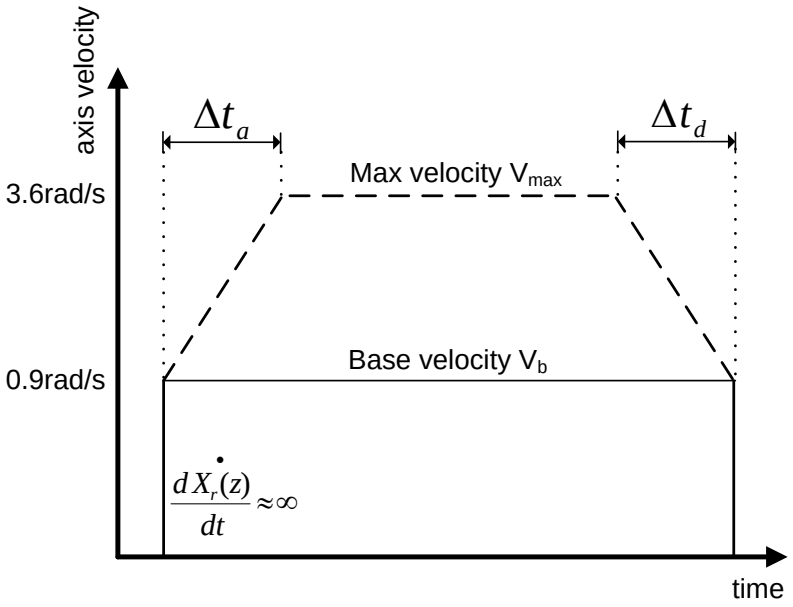

Fig. 3. Approximate velocity-time profile of the robot for with negligible load characteristics and moment of Inertia, $I_c \approx 0$

To simplify the analysis the current development of the prototype robot is only operated at base speeds resulting in an effective instantaneous acceleration and deceleration. This simplified dynamic behaviour of the robot can be modelled as a saturation function, *f(v)* where *v* is the input velocity command. The function *f(v)* is represented graphically in Figure 4 and is defined as,

$$f(v) = \begin{Bmatrix} v & if & -0.03 < v < 0.03 \\ 0.03 & if & v \geq 0.03 \\ -0.03 & if & v \leq -0.03 \end{Bmatrix}$$

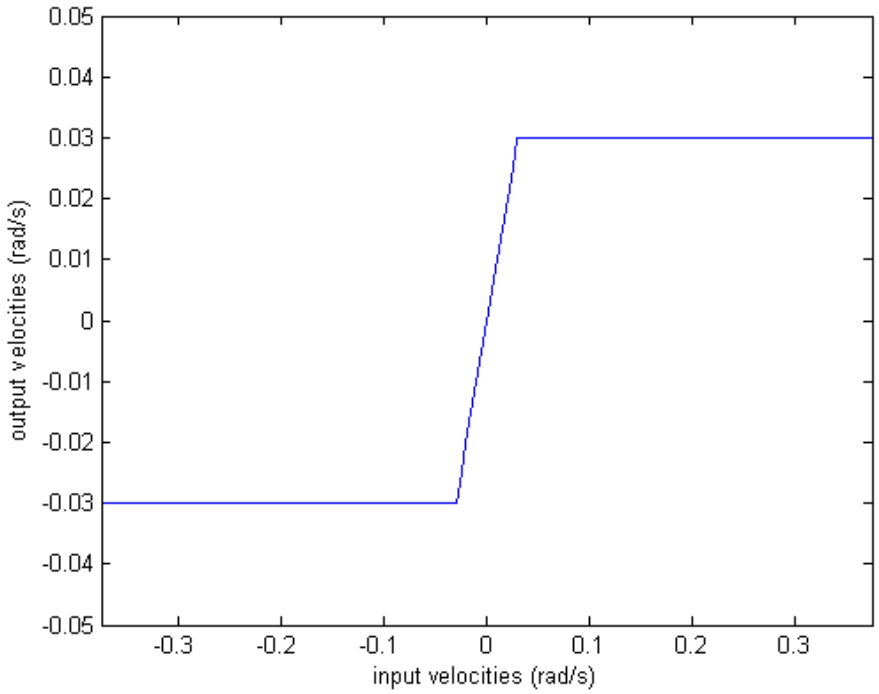

Fig. 4. Simplified robot dynamic model

Analysis of system modelling

The model developed in the previous section can be written as a closed loop transfer function that describes the image plane pixel error $E_p(z)$ for a given target motion $X_t(z)$,

$$\frac{E_p(z)}{X_t(z)} = \frac{V(z)}{1+V(z)R(z)D(z)}$$
$$= \frac{K_{lens}(z-1)}{z^2 - z + K_p / K_{lens}}$$

To analyse the stability of the closed loop system a root locus is drawn as shown in Figure 6 with the feedback proportional gain K_p of 1.

Note that the robot dynamics term is not included in the above transfer function. Due to the non-linearity of the function approximation, *f(v)*, the assumption of linearity in calculating the transfer function is invalidated. It is found that using a proportional controller only the robot dynamics will have no effect on the stability of the system. The term will only increase the amplitude of the oscillations shown in Figure 5 (dashed) while remaining marginally stable for a gain of 1. Therefore, the simplified dynamic model of the robot shown in Figure 5 will be excluded from the stability calculations.

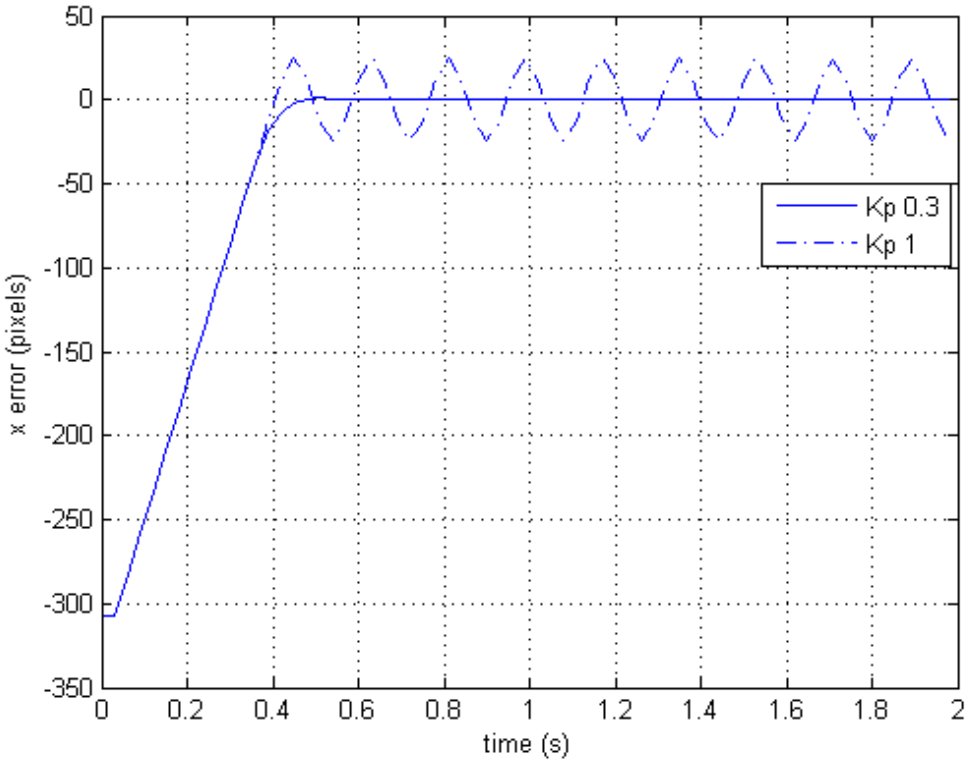

Fig.5. Simulated model response of Pixel Error E(z) to a 0.375 radian step input. The figure shows the critically damped and oscillatory response of the system for a proportional gain K_p 0.3 (solid) and K_p 1(dashed) respectively

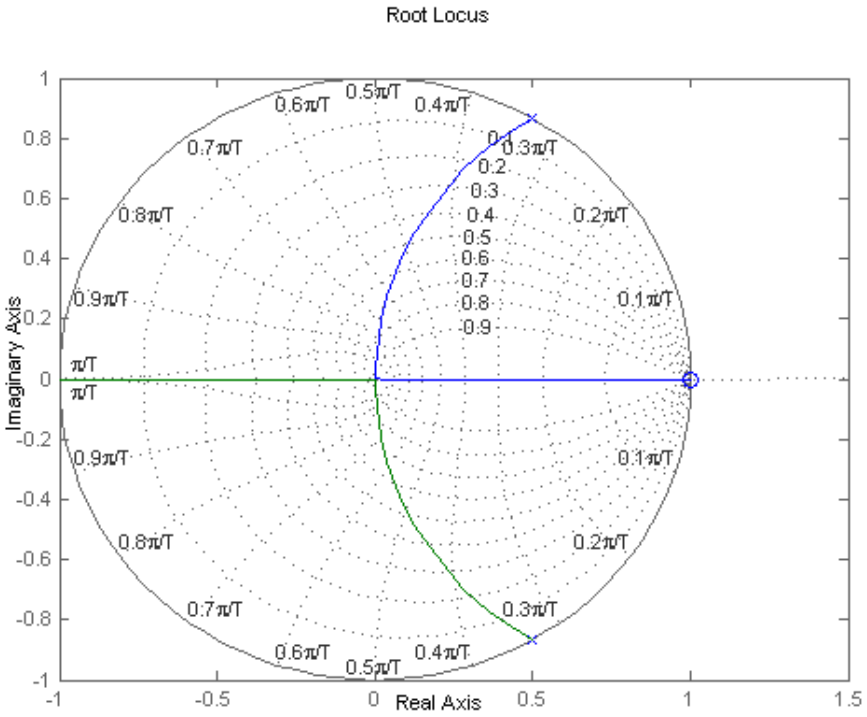

Fig. 6. Root locus plot for the closed loop visual servoing system with a feedback proportional gain K_p of 1.

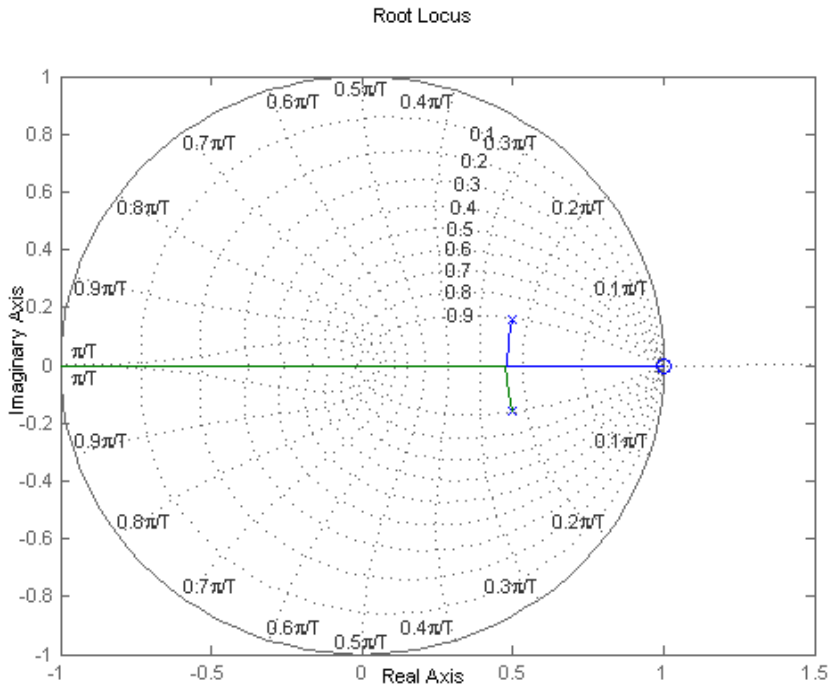

Fig. 7. Root locus plot for the closed loop visual servoing system with a feedback proportional gain K_p of 0.3. Note that the stability of the system increase at the cost of tracking performance

It is apparent from the root locus plot in Figure 6, that with a proportional gain K_p of 1 the complex poles of the closed loop system are on the unit circle. This results in a system that oscillates about a desired target location by the change in angle made by the robot in one sample period. The marginal stability in a closed loop visual servoing system is caused primarily by the latency in vision and is well documented by Corke *et al.* [8]. The following section describes the timing relationship of the system and discusses the reason for latency in this particular setup.

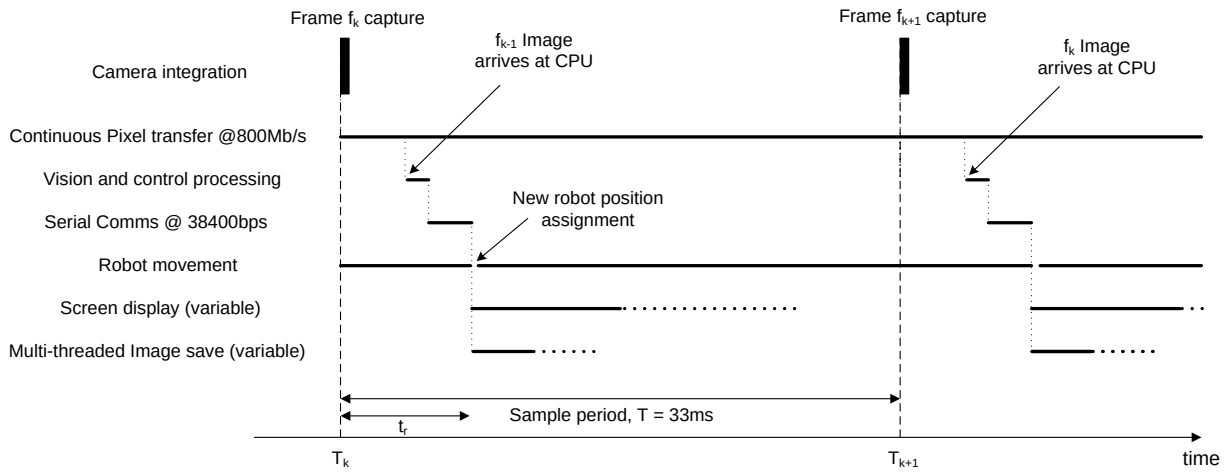

Fig. 8. System timing diagram for a large initial target movement where the robot axes cannot achieve the required velocities before the next shutter event. Note that the timing of each task is approximate and only provides a general idea about the times required for various tasks.

This instability is compensated at the expense of system performance. To obtain critical damping for a step change in the target angle, the gain K_p is set to 0.3. Figure 7 shows the change in the location of the poles with the difference between the two responses shown in Figure 5.

This configuration can achieve zero pixel error in approximately 420ms for a maximum step input, i.e. stationary target with offset from the centre of the image by 320 pixels when running on 640x480 pixel resolution.

System Timing

The behaviour and stability of this visual servoing system depends on the timing and completion of various tasks. Figure 8 shows the approximate duty cycle of tasks over a sample period *T*. It is clear that the primary cause of latency in this system is the pixel transfer which occurs between the camera and the host computer. The image processing algorithm and communication between the software and the robot takes approximately 4ms and is relatively small when compared to the delay caused by the transfer of pixels. Image f_k only arrives at the CPU after the f_{k+1} camera shutter event has elapsed, i.e. the image that is processed to determine robot angles uses target information out dated by a single frame. The latency was found to increase up to three sample periods when the number of cameras on the same bus or single camera resolution was increased[1].

For a high velocity target, the robot may not achieve sufficient rotation to keep the target centred in the frame for a given sample period. In this case the pose of the robot may still be changing while the subsequent frame is being captured as shown in Figure 8. This causes a short period of time, t_r where the robot rotation is not accounted for until the next frame and results in a slight overshoot of the robot position. The angle overshoot can be approximated as a rotational movement made by that axis in time t_r before the new robot position angles become available.

[1]The three sample period delay also includes a long shutter opening of the camera. All modeling and experiments are conducted using an ideal sample.

The vision algorithm and the control are only activated by the use of a single mouse click event. The click serves as a manual target detection task which activates the vision and control processing on each of the following frames. The initial click may occur stochastically between a shutter event[1] and cause variable robot axis movement for the initial 'tracking activated' sample period. Following this initial frame the robot axes movements are allowed to change positions for a complete 33ms allowing fixed times for the robot to move. This validates the robot movement of 0.03rad/33ms assumed earlier to form a simplified robot dynamic model.

Experiments

This visual servoing system is tested using various target trajectories to illustrate the tracking performance of the system. Comparison between the actual system and simulations are also discussed to illustrate the accuracy of the simulation model. The assumption made during the design stages especially in approximating the moment of inertia to zero is validated by the similarities in the response of the simulation when compared to the actual system.

Figure 9 (top) shows the tracking error performance for a sinusoidal target trajectory for the pan axis. Pendulum motion of the target was set at an angular velocity of approximately 2.5 rad/s, with peak amplitude of 0.25 radians. The system fixates on the target with a maximum

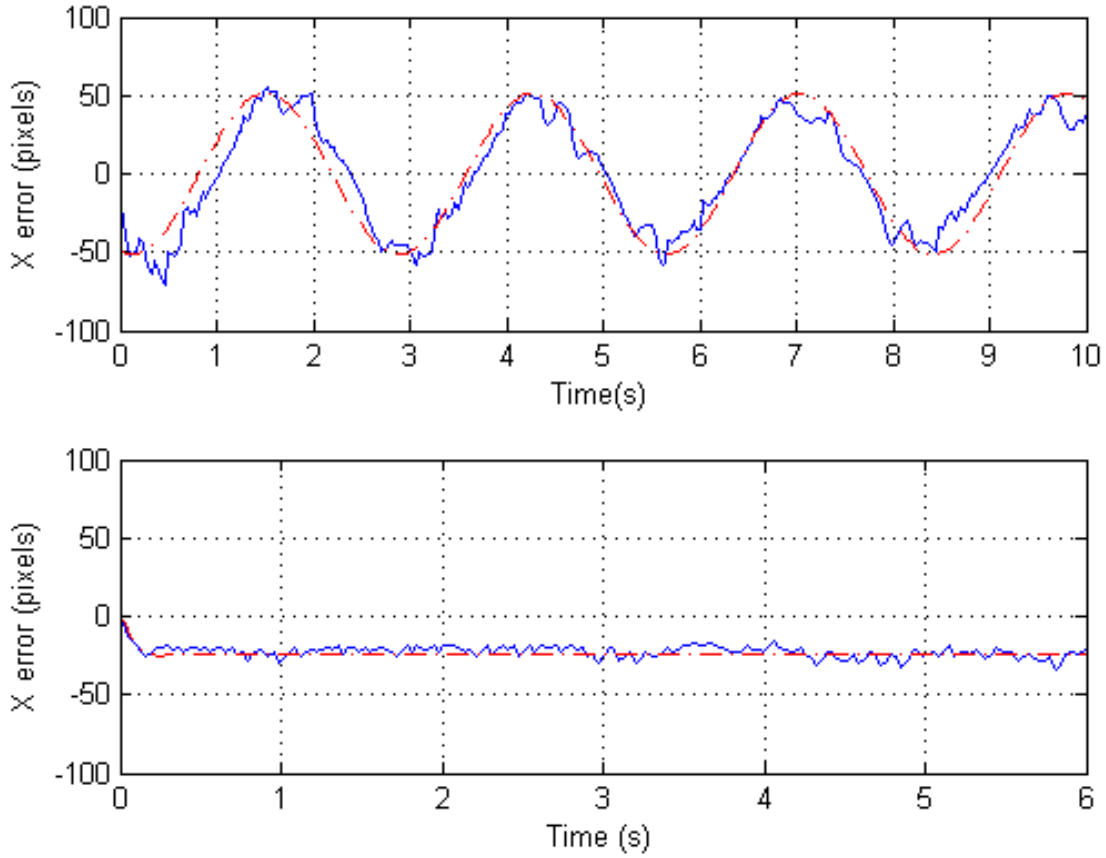

Fig. 9. Response of the system(solid) and simulation (dashed) to different target trajectories. The plots show the x axis pixel error response of the system for a constant velocity (bottom) and a sinusoidal (top) target trajectory at 640x480 pixel resolution. The target movement is approximately 0.25 radians in amplitude and with a frequency of 2rad/s for sinusoidal and 0.5rad/s continuous for constant velocity target trajectory.

[1]Shutter event is referred to the opening and closing of the camera shutter

error of 50 pixels when running at a 640x480 pixel resolution. Note that when the pixel resolution is increased the error increases due to higher resolution and also due to the increase in the number of pixels to be transferred from the camera to the CPU causing increased latency in the vision system.

Experiments were also conducted using a constant velocity motion of the target set at 0.5rad/s. A tracking steady state error of about 23 pixels is obtained when a single camera is operated at 640x480 pixel resolution.

Conclusion

This paper discusses the implementation of a visual feedback control scheme that is being developed for tracking and obtaining thermal radiation data of HIFiRE vehicles. The initial development of the feedback control scheme shows the advantages of using visual servoing over passive target tracking methods and manual crew operations. The scheme uses much simpler equipment and system design to perform the tracking task. The most significant factor affecting the performance of the system is the delay caused by the latency in the vision system.

To reduce the steady state error in the constant velocity and peak to peak error in the sinusoidal motion target tracking can be reduced significantly using feedforward control architecture. This technique uses estimation to predict current target location based on the previous movements and overcome the lag caused by latency of the vision system discussed earlier. Such feedforward control design can be implemented using existing equipment in the final ground based system used for the observation. It is anticipated that in future, the observation equipment would be installed on an unmanned airborne platform that could fly closer to the vehicle trajectory and obtain high resolution thermal imagery and emission spectroscopy autonomously.

References

1. B.D.Lucas and T.Kanade, “An image registration technique with an application to stereo vision”, in *Proceedings International Joint Conference on Artificial Intelligence*, 1981, pp.674-679
2. Roger Y.Tsai and Reimar K.Lenz, “A New Technique for Fully Autonomous and Efficient 3D Robotics Hand/Eye Calibration”, *IEEE transaction on Robotics and Automation*, vol 5, np.3, June 1989
3. J.T.Feddema, C.S.G Lee, and O.R.Mitchell, “Weighted Selection of Image Features for Resolved Rate Visual Feedback Control”, *IEEE transaction in Robotics and Automation*, vol 7, pp.31-47 Feb 1991
4. N.P.Papanikolopoulos, P.K Khosla, and T.Kanade, “Visual tracking of a moving target by a camera mounted on a robot: A combination of vision and control”, *IEEE transaction in Robotics and Automation*, vol 9, no.1, pp.14-35 1993
5. R.M.Haralick and L.G. Shapiro, “Computer and Robot Vision”, Reading, MA: Addison-Wesley, 1993
6. Peter I.Corke, “High Performance Visual Closed Loop Robot Control”, *PhD dissertation*, University of Melbourne, Department of Mechanical and Manufacturing Engineering, July 1994
7. Seth Hutchinson, Gregory D.Hager and, Peter I.Corke, “A Tutorial on Visual Servo

Control", *IEEE transactions on Robotics and Automation*, vol. 12 no. 5, October 1996
8. Peter I.Corke and Malcolm C.Good 1996, "Dynamic Effects in Visual Servoing Closed-Loop System", *IEEE transaction in Robotics and Automation*, vol 12, no.5, p671-683 October 1996
9. Alessandro De Luca, Giuseppe Oriolo and Paolo Robuffo Giordano, "Feature Depth Observation for Image-based Visual Servoing: Theory Experiments", *The International Journal of Robotics Research* 2008;27;1093
10. Odile Bourquardez, Robert Mahony, Nicolas Guenard, Franc¸ois Chaumette, Tarek Hamel, and Laurent Eck, "Image based Visual Servo Control of the Translation Kinematics of a Quadrotor Aerial Vehicle", *IEEE transaction in Robotics and Automation*, vol 25, no.3, June 2009
11. Thomas J.Horvath, Deborah M.Tomek, Karen T.Berger, Scott C.Splinter, Joseph N.Zalameda, Paul W.Krasa, Steve Tack, Richard J.Schwartz, DavidM.Gibson, and Alan Tietjen, "The HYTHIRM Project: Flight Thermography of the Space Shuttle During Hypersonic Re-entry", AIAA 2010-241, *48th AIAA Aerospace Science Meeting* Jan 4-7, Orlando, Florida, 2010
12. Steve Tack, Deborah M.Tomek, Thomas J.Horvath, Harry A.Verstynen, Edward J.Shea, "Cast Glance Near Infrared Imaging Observation of the Space Shuttle During Hypersonic Re-entry", 2010-243, *48th AIAA Aerospace Science Meeting*, Jan 4-7, Orlando, Florida, 2010
13. Joseph N.Zalameda, Alan B.Tietjen, Thomas J. Horvath, Deborah M.Tomek, David M.Gibbs, Jeff C.Taylor, Steve Tack, Brett C.Bush, David Mercer, Edward J.Shea, "Application of a Near Infrared Imaging System for Thermographic Imaging of the Space Shuttle during Hypersonic Re-entry", 2010-245, *48th AIAA Aerospace Science Meeting* Jan 4-7, Orlando, Florida, 2010